Trans. Tianjin Univ. 2014, 20: 091−096
DOI 10.1007/s12209-014-2233-7

Comparative Study on the Pyrolysis Behaviors of Corn Stalk and Pine Sawdust Using TG-MS*

Zhao Yunpeng（赵云鹏），Ding Man（丁　曼），Dou Youquan（窦有权），
Fan Xing（樊　星），Wang Yuelun（王月伦），Wei Xianyong（魏贤勇）
（School of Chemical Engineering and Technology, China University of Mining and Technology, Xuzhou 221116, China）

© Tianjin University and Springer-Verlag Berlin Heidelberg 2014

Abstract：The pyrolysis behaviors of corn stalk（CS）and pine sawdust（PS）were investigated with thermogravimetry-mass spectroscopy（TG-MS）. The peak temperature of PS was higher and the main decomposition region shifted to higher temperature compared with CS, which implied that the hemicellulose and cellulose of PS were more thermally stable than those of CS. However, the hemicellulose and cellulose of PS were more easily decomposed into gaseous products than those of CS during pyrolysis. The pyrolysis process of biomass can be described by a two-step independent first-order kinetic model. This fundamental study provides a basic insight into the biomass pyrolysis, which is beneficial for understanding the pyrolysis mechanism of biomass and developing an advanced thermal process for effective utilization of biomass.

Keywords：biomass; pyrolysis; kinetics; TG-MS

Due to the rapid depletion of fossil resources and the problem of greenhouse gas emissions, much attention has been focused on alternative fuels and chemicals produced from biomass, especially from agricultural and forestry residues for their cheapness and abundance[1]. In various processes, pyrolysis is now considered to be a promising technique of utilizing biomass, which converts the lignocellulosic materials into bio-oil, char and gas[2]. The bio-oil and gas can be used as a fuel or a feedstock for chemicals, and char can be used as a domestic fuel, a feedstock of activated carbon, or a reducing agent in metallurgy[3, 4]. Additionally, pyrolysis is an important intermediate stage of major thermochemical processes of solid fuel, such as combustion, gasification, carbonization and liquefaction[5]. Therefore, understanding the pyrolysis behavior of biomass is of benefit to the conversion of biomass to value-added products and the identification of reaction mechanism in thermochemical conversion of biomass.

Understanding pyrolysis kinetics is important for effective design, operation and control of thermochemical conversion equipments and processes[6, 7]. Thermogravimetric analysis（TGA）has been widely applied to identifying the reactivity and kinetics of biomass pyrolysis, but it cannot provide information about the nature of the evolved volatile components[8]. The technology of TGA coupled with mass spectrometry（MS）is able to afford the real-time and sensitive detection of evolved gases. The pyrolysis behavior of various biomass feedstocks has been widely investigated with TG-MS in recent years[9-13]. However, biomass pyrolysis is an extremely complex process, undergoing a series of reactions and subjected to the influence of various factors.

The aim of the present work is to compare the differences between corn stalk（CS）and pine sawdust（PS）in the pyrolysis reactivity and evolution profiles of gaseous products. Results from this study contribute to understanding the pyrolysis mechanism of biomass, and provide a comparison of different feedstocks and their potential for use and upgrading.

1 Experimental

1.1 Materials

CS（with leaves removed）was obtained from Xuzhou City, Jiangsu Province, China, and PS was obtained from a wooden factory of Dalian City, Liaoning

---

Accepted date: 2013-08-09.

*Supported by the National Basic Research Program of China (“973” Program, No. 2012CB215302), National Natural Science Foundation of China (No. 21206188 and No. 21106177), China Postdoctoral Science Foundation (No. 2012M511339) and Fundamental Research Funds for the Central Universities (China University of Mining and Technology, No. 2011QNA23).

Zhao Yunpeng, born in 1981, male, lecturer.
Correspondence to Zhao Yunpeng, E-mail: yunpengzhao2009@163.com.

Province, China. The samples were ground in a Wiley mill and screened with < 80 mesh for the experiments. Tab. 1 lists the proximate, ultimate, and group composition analyses of samples.

Tab. 1 Proximate, ultimate, and group composition analyses of CS and PS (wt%)

Sample	Proximate analysis			Ultimate analysis (dry ash-free basis)					Group composition (dry basis)		
	M_{ad}	A_d	V_{daf}	C	H	N	S	O^a	Lignin	Cellulose	Hemicellulose
CS	7.93	12.12	78.88	50.32	9.51	1.24	0.16	38.77	20.18	24.85	32.20
PS	5.88	1.46	85.84	49.52	6.49	0.05	0.05	43.89	30.15	39.54	20.61

Note: Superscript ^{a} means that the content of O is obtained by difference; M_{ad} represents moisture content (air dry basis); A_d represents ash content (dry basis); V_{daf} represents volatile content (dry ash-free basis).

1.2 Fourier transform infrared spectroscopy (FTIR) analysis

Functional groups of biomass samples were measured by an EQUINOX55 spectrophotometer using KBr pellet technique. The spectra were recorded from 4 000 to 400 cm^{-1} at 2 cm^{-1} resolution.

1.3 Pyrolysis experiments

The pyrolysis experiments were performed using a Mettler Toledo TGA/SDTA851^e thermogravimetry analyzer. During the experiments, about 10 mg of sample was placed in a ceramic crucible and heated from 25 to 850 ℃ with a heating rate of 10 ℃/min using argon as carrier gas at a constant flow rate of 60 mL/min. A quadrupole mass spectrometer (GSD-301 T3, MS) coupled to the thermogravimetry analyzer was used for the evolved gas analysis. To avoid secondary reactions, a probe was placed very close to the sample pan of the themogravimetry analyzer in the direction of gas flow. The transfer lines between the TGA and the MS were heated to 180 ℃ in order to avoid cold spots and thus prevent the condensation of the gaseous products. The signals for *m*/*z* 2, 16, 18, 44, 64 and 78 were continuously detected.

2 Results and discussion

2.1 FTIR analysis

As shown in Fig. 1, the FTIR spectrum of CS is similar to that of PS except for the different absorption intensities of some functional groups. Both of CS and PS have strong intensities of peaks attributed to the O—H stretching vibration (3 000—3 600 cm^{-1}) and C—O bending vibration (1 050 cm^{-1}) of glycosidic linkages[14]. The stretching vibration (2 800—3 000 cm^{-1}) and bending vibration (1 350—1470 cm^{-1}) of C—H indicate the presence of aliphatic side chain, while weak absorption band at 896 cm^{-1} is ascribed to the C—H deformation vibration of β-(1-4)-glucosidic linkages [14]. The intensity of absorption peak attributed to C=O stretching vibration (1 735 cm^{-1}) from PS is higher than that from CS, suggesting that the content of ketone, aldehyde, ester, or carboxylic acid groups in PS is more than that of CS [15]. Moreover, the intensity of aromatic skeletal vibration at 1 508 cm^{-1} and 1 650 cm^{-1} from PS is higher than that of CS, which is in accord with the lignin content in PS [16, 17]. In addition, the absorption peaks at 1 250 cm^{-1} and 1 160 cm^{-1} originate from the C—O—C stretching vibration in guaiacyl rings and C—H plane deformation vibration in syringyl unit, respectively[14, 17].

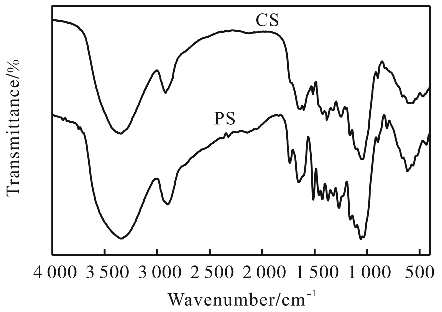

Fig. 1 FTIR spectra of biomass feedstocks

2.2 TGA results of biomass feedstocks

Thermogravimetry (TG, wt%) curves and differential thermogravimetry (DTG, %/℃) curves of biomass are shown in Fig. 2. Compared with CS, the peak temperature of PS is higher and the main decomposition region shifts to higher temperature, implying that the hemicellulose and cellulose of PS are more thermally stable than those of CS. However, the weight loss up to 400 ℃ and the maximum weight loss rate of PS are obviously higher than those of CS, which is possibly ascribed to the higher cellulose content of PS (Tab. 1). The decomposition region of lignin occurs over a broad range of temperature, therefore, the flat tailing section at higher temperatures is ascribed to the decomposition of lignin[7, 18, 19]. It can be seen that at 600 ℃, the mass losses of CS and PS are 74.77% and 78.71%, respectively, which is coincident with the results that the volatile matter content of CS is lower than that of PS (Tab. 1).

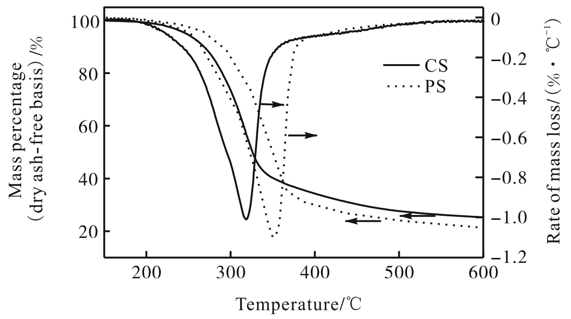

Fig. 2 TG/DTG curves of biomass samples

2.3 Kinetics of biomass pyrolysis

In many investigations, the pyrolysis of biomass was assumed to be the first-order reaction [8, 16, 20]. Therefore, the reaction equation of biomass pyrolysis can simply be expressed as the following formula:

$$-\frac{\mathrm{d}x}{\mathrm{d}t}=A\exp(-\frac{E}{RT})(1-x) \qquad (1)$$

where A is pre-exponential factor; E is activation energy; T is temperature; t is time; and x is the weight loss fraction of pyrolysis conversion which can be calculated by

$$x=\frac{W_{\mathrm{o}}-W_t}{W_{\mathrm{o}}-W_{\mathrm{f}}} \qquad (2)$$

where W_0 is the original mass of the test sample; W_t is the mass at time t or temperature T; and W_{f} is the final mass at the end of pyrolysis.

For a constant heating rate H during pyrolysis, $H=\mathrm{d}T/\mathrm{d}t$, Eq. (1) is integrated by using Coats-Redfern integration method as follows [21]:

$$\ln[\frac{-\ln(1-x)}{T^2}]=\ln[\frac{AR}{HE}(1-\frac{2RT}{E})]-\frac{E}{RT} \qquad (3)$$

If the pyrolysis process can be assumed as the first-order reaction, a straight line may be obtained when the left side of Eq. (3) is plotted versus $1/T$. From the slope, $-E/R$, the activation energy E can be determined. From the intercept $\ln[\frac{AR}{HE}(1-\frac{2RT}{E})]$, using the temperature at which $W_t=(W_{\mathrm{o}}-W_{\mathrm{f}})/2$, the pre-exponential factor A can also be determined.

Fig. 3 (a) shows the typical plot of $\ln[-\ln(1-x)/T^2]$ versus $1/T$, indicating that the reaction of biomass pyrolysis cannot be described by one consecutive first-order reaction. It seems to be two independent first-order reactions at different temperature regions. Therefore, the two independent first-order reactions were tried to describe the process of coal pyrolysis, which means that Eq. (1) is applied separately to the two stages, and that the conversion x is recalculated for each reaction. Fig. 3 (b) shows a typical result taking CS as an example. From the slope and intercept of each line, the values of E and A can be obtained for different stages. Tab. 2 shows the kinetic parameters determined by this method and the characteristic temperatures of pyrolysis. The kinetic parameters are calculated in the range of x from 5% to 95% which represents the main pyrolysis region. The good correlation coefficient indicated that the two independent first-order kinetics models fit the experimental data very well.

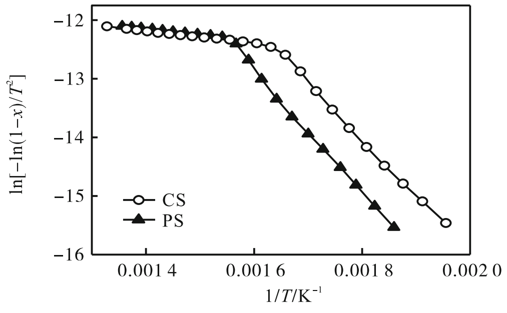

(a) One first-order reaction

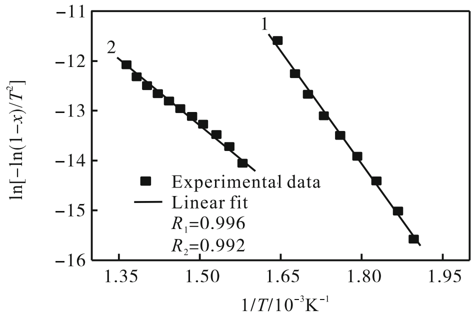

(b) Two independent first-order reactions of CS

Fig. 3 ln[−ln(1−x)/T^2] vs. 1/T of biomass pyrolysis

The activation energy obtained using this method is between 86 and 129 kJ/mol. Hirschfelder [22] proposed an activation energy formula:

$$E=b\sum D \qquad (4)$$

where b is constant; D is the activation energy of one cleavage bond; and $\sum D$ is the total activation energy of all cleavage bonds during pyrolysis. It implies that the total activation energy is related to either the activation energy of sole cleavage bond or the number of cleavage bonds. During biomass pyrolysis, the cleavage of sole bonds in lignin was possibly more difficult than that in hemicellulose and cellulose, but the number of cleavage bonds in lignin was significantly less than that in hemicellulose and cellulose. Therefore, it was not difficult to understand that the activation energy in the first stage was higher than that in the second stage during biomass pyrolysis. However, the pre-exponential factor, another impact factor for reaction rate, was obviously higher in the first stage than that in the second stage, which indicated a higher decomposition rate of hemicellulose and cellulose. Additionally, the lignin content in CS was obviously lower than that in PS (Tab. 1), which suggested that the number of cleavage bonds in the lignin of CS was obviously lower than that in the lignin of PS. Therefore, the activation energy of CS in the first stage (125.0 kJ/mol) was significantly higher than that in the second stage (70.3 kJ/mol), while the activation energy of PS in the first stage (88.3 kJ/mol) was almost equal to that in the second stage (86.6 kJ/mol).

Tab. 2 Kinetic parameters and characteristic temperatures of biomass pyrolysis

Sample	T/℃	x/%	$(dW/dt)_{max}$/(% · min^{-1})	T_p/℃	E/(kJ · mol^{-1})	A/min^{-1}	Correlation coefficient
CS	238—340	5—77	1.0	318	125.0	6.5×10^{10}	0.996
	340—471	77—95			70.3	1.5×10^{5}	0.992
PS	264—363	5—80	1.1	351	88.3	6.7×10^{7}	0.994
	363—465	80—95			86.6	9.8×10^{5}	0.995

Note: T_p represents peak temperature in DTG curve.

Compared with PS, the first stage of CS was located in a lower temperature region (238—340 ℃), which indicated that the hemicellulose and cellulose of CS were more easily decomposed than those of PS. Nevertheless, the activation energy and pre-exponential factor of CS in the first stage were higher than those of PS, suggesting that there were more cleavage bonds in the hemicellulose and cellulose of CS. On the contrary, the activation energy and pre-exponential factor of PS in the second stage were higher than those of CS, implying more cleavage bonds in the lignin of PS during pyrolysis, which was in accord with the higher gas evolution intensity of PS in high temperature region (Fig. 4).

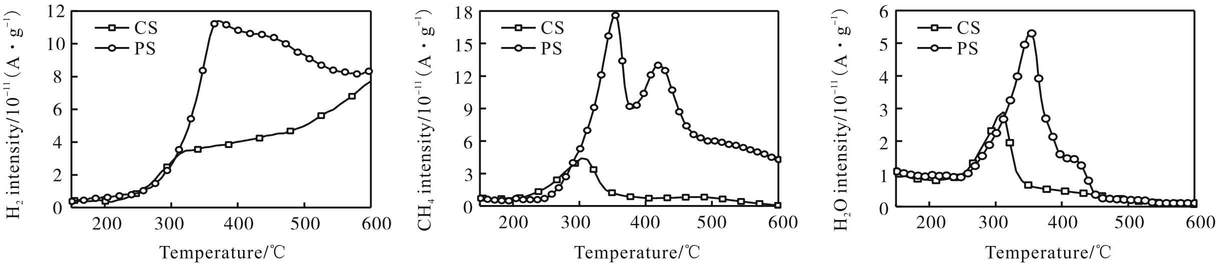

(a) H_2 (b) CH_4 (c) H_2O

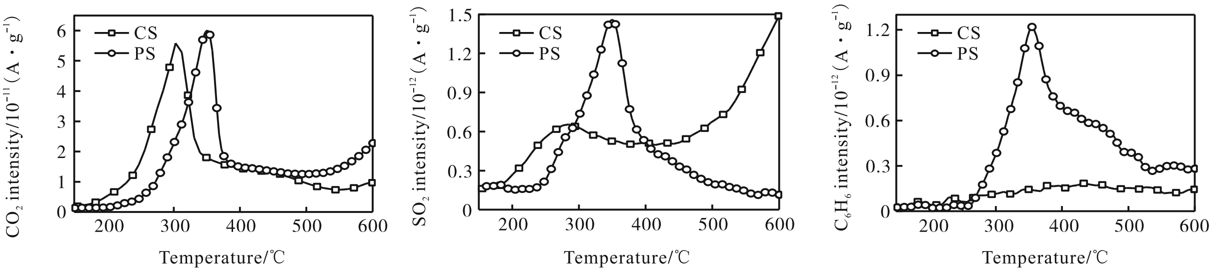

(d) CO_2 (e) SO_2 (f) C_6H_6

Fig. 4 Evolution curves of gas products during pyrolysis of biomass

2.4 Gas evolution profile

By means of TG-MS analysis, thermogravimetric data can be obtained as well as the information about the gas evolution profile. Fig. 4 shows the evolution curves of H_2 (m/z 2), CH_4 (m/z 16), H_2O (m/z 18), CO_2 (m/z 44), SO_2 (m/z 64) and C_6H_6 (m/z 78) during the pyrolysis of biomass. It can be clearly seen that the formation of most of gas products is well accompanied by the sharp decomposition of biomass shown in the TG/DTG curves. Interestingly, for most of gas products, their evolution intensity from PS is higher than that from CS, which implies that the volatile matter in PS is easily decomposed into gases.

The evolution of H_2 starts at about 200 ℃ and the evolution intensity sharply increases with the increase of temperature until it reaches the inflection point at the temperature T_p. Over T_p, H_2 evolution intensity of CS consistently increases with temperature, whereas H_2 evolution intensity of PS significantly decreases until 475 ℃, and one shoulder peak occurs between 400 and 500 ℃. At low temperature, the evolution of H_2 is ascribed to the degradation of cellulose and hemicellulose, while it is generated from the condensation of aromatic and hydroaromatic structures or the decomposition of heterocyclic compounds at high temperature [23]. Additionally, compared with hemicellulose and lignin, the pyrolysis of cellulose produces more H_2 [8]. Therefore, PS owns higher H_2 evolution intensity possibly due to its higher cellulose content than CS (Tab. 2). CH_4 is mainly generated from ·CH_3 and ·CH_2 radicals, which are stabilized by non-aromatic hydrogen at low temperature and from the reaction of carbon with hydrogen at high temperature[24]. In accord with its higher H_2 evolution intensity, CH_4 evolution intensity of PS is higher than that of CS, and there is an extra evolution peak at around 420 ℃ except the peak located at around T_p.

The evolution of water is generally attributed to the esterification and dehydration reaction of phenolic hydroxyl groups in biomass[23]. Higher peak temperature of PS suggestes that the phenolic hydroxyl groups in PS are more stable than those in CS, while higher water evolution intensity of PS is ascribed to its higher content of phenolic hydroxyl groups and more ·H radical produced during pyrolysis which could stabilize more ·OH radical to produce water. Aliphatic and aromatic carboxyl groups could be decomposed into CO_2 below 200 ℃, but only high temperature could lead to the decomposition of stable ether, quinone, oxygen-bearing heterocycles or carbonates[25]. Therefore, the CO_2 evolution curves distribute in a wide temperature range. The lower initial evolution and peak temperature for CS indicates that the oxygen-containing functional groups in CS are more easily cleaved than those in PS during pyrolysis, while the evolution intensity of CO_2 from PS obviously increases when the temperature is above 500 ℃, indicating that there are many stable oxygen-containing groups in PS.

Although the sulfur content is very low in biomass, obvious evolution profiles of SO_2 were identified using TG-MS, and the evolution curve of CS is significantly different from that of PS. As for CS, SO_2 starts to evolve below 200 ℃, and gets a maximum at about 280 ℃, then slightly decreases as the temperature increases from 280 to 450 ℃. Over 450 ℃, the evolution intensity of SO_2 from CS sharply increases with temperature. As for PS, the initial temperature and peak temperature of SO_2 are higher than those of CS, and the evolution intensity decreases when the temperature is above 350 ℃. Few references about SO_2 evolution profile during biomass pyrolysis have been found, while the evolution of SO_2 during coal pyrolysis at low temperature is mainly related to the decomposition of aliphatic and unstable aromatic sulfur (such as thiols, disulfide and aryl-aryl sulfides), and at high temperature it originates from the decomposition of some stable cyclic and aromatic sulfur, dibenzothiophen and thiophenes, etc. These results indicate that stable cyclic and aromatic sulfur, dibenzothiophen and thiophenes possibly exist in CS except aliphatic and unstable aromatic sulfur. Obvious evolution peak of C_6H_6 is detected for PS, while there is little evolution signal for CS, which might be attributed to the high cellulose content of PS.

3 Conclusions

The pyrolysis reactivity and gas evolution profile were significantly different between CS and PS. The hemicellulose and cellulose of PS were more thermal stable than those of CS, while they were decomposed into gas products more easily than those of CS during pyrolysis. The pyrolysis process of biomass studied can be described by a two-step independent first-order kinetic model, and activation energy was related to either the activation energy of sole cleavage bond or the number of cleavage bonds.

References

[1] Kim S W, Koo B S, Ryu J W *et al*. Bio-oil from the pyrolysis of palm and Jatropha wastes in a fluidized bed [J]. *Fuel Processing Technology*, 2013, 108: 118-124.

[2] Bridgwater A V, Meier D, Radlein D. An overview of fast pyrolysis of biomass[J]. *Organic Geochemistry*, 1999, 30 (12): 1479-1493.

[3] Fisher T, Hajaligol M, Waymack B *et al*. Pyrolysis behavior and kinetics of biomass derived materials [J]. *Journal of Analytical and Applied Pyrolysis*, 2002, 62 (2): 331-349.

[4] Demirbas M F, Bala M. Recent advances on the production and utilization trends of bio-fuels: A global perspective [J]. *Energy Conversion and Management*, 2006, 47 (15/16): 2371-2381.

[5] Zhao Y P, Hu H Q, Jin L J *et al*. Pyrolysis behavior of weakly reductive coals from Northwest China [J]. *Energy Fuels*, 2009, 23 (1): 870-875.

［6］ Li Z Q, Zhao W, Meng B H *et al*. Kinetic study of corn straw pyrolysis: Comparison of two different three-pseudocomponent models［J］. *Bioresource Technology*, 2008, 99（16）: 7616-7622.

［7］ Fasina O, Littlefield B. TG-FTIR analysis of pecan shells thermal decomposition［J］. *Fuel Processing Technology*, 2012, 102（1）: 61-66.

［8］ Huang Y F, Kuan W H, Chiueh P T *et al*. Pyrolysis of biomass by thermal analysis-mass spectrometry（TA-MS）［J］. *Bioresource Technology*, 2011, 102（3）: 3527-3534.

［9］ Szabo P, Varhegyi G, Till F *et al*. Thermogravimetric/mass spectrometric characterization of two energy crops, *Arundo donax* and *Miscanthus sinensis*［J］. *Journal of Analytical and Applied Pyrolysis*, 1996, 36（2）: 179-190.

［10］ Worasuwannarak N, Sonobe T, Tanthapanichakoon W. Pyrolysis behaviors of rice straw, rice husk, and corncob by TG-MS technique［J］. *Journal of Analytical and Applied Pyrolysis*, 2007, 78（2）: 265-271.

［11］ Meszaros E, Jakab E, Varhegyi G. TG/MS, Py-GC/MS and THM-GC/MS study of the composition and thermal behavior of extractive components of Robinia pseudoacacia［J］. *Journal of Analytical and Applied Pyrolysis*, 2007, 79（1/2）: 61-70.

［12］ Gomez C J, Meszaros E, Jakab E *et al*. Thermogravimetry/mass spectrometry study of woody residues and an herbaceous biomass crop using PICA techniques［J］. *Journal of Analytical and Applied Pyrolysis*, 2007, 80（2）: 416-426.

［13］ Barneto A G, Carmona J A, Alfonso J E M *et al*. Use of thermogravimetry/mass spectrometry analysis to explain the origin of volatiles produced during biomass pyrolysis［J］. *Industry & Engineering Chemistry Research*, 2009, 48（15）: 7430-7436.

［14］ Lv G J, Wu S B. Analytical pyrolysis studies of corn stalk and its three main components by TG-MS and Py-GC/MS［J］. *Journal of Analytical and Applied Pyrolysis*, 2012, 97: 11-18.

［15］ Hu J, Shen D K, Xiao R *et al*. Free-radical analysis on thermochemical transformation of lignin to phenolic compounds［J］. *Energy & Fuel*s, 2013, 27（1）: 285-293.

［16］ Zhang A Q, Zhao Z L, Chang S *et al*. Effect of torrefaction temperature on product distribution from two-staged pyrolysis of biomass［J］. *Energy & Fuel*s, 2012, 26（4）: 2968-2974.

［17］ Aziz S M A, Wahi R, Ngaini Z *et al*. Bio-oil from microwave pyrolysis of agricultural wastes［J］. *Fuel Processing Technology*, 2013, 106（2）: 744-750.

［18］ Yang H, Yan R, Chen H *et al*. Characteristics of hemicellulose, cellulose and lignin pyrolysis［J］. *Fuel*, 2007, 86（12/13）: 1781-1788.

［19］ Greenhalf C E, Nowakowski D J, Harms A B. A comparative study of straw, perennial grasses and hardwoods in terms of fast pyrolysis products［J］. *Fuel*, 2013, 108（6）: 216-230.

［20］ Zhao Y P, Hu H Q, Jin L J *et al*. Pyrolysis behavior of macerals from weakly reductive coals［J］. *Energy & Fuels*, 2010, 24（12）: 6314-6320.

［21］ Coats A, Redfern J P. Kinetics parameters from thermogravimetric data［J］. *Nature*, 1964, 201（4）: 68-69.

［22］ Hirschfelder J O. Semi-empirical calculations of activation energies［J］. *The Journal of Chemical Physics*, 1941, 9（8）: 645-654.

［23］ Widyawati M, Church T L, Florin N H *et al*. Hydrogen synthesis from biomass pyrolysis with in situ carbon dioxide capture using calcium oxide［J］. *International Journal of Hydrogen Energy*, 2011, 36（8）: 4800-4813.

［24］ Shen D K, Gu S, Luo K H *et al*. The pyrolytic degradation of wood-derived lignin from pulping process［J］. *Bioresoure Technology*, 2010, 101（15）: 6136-6146.

［25］ Bilba K, Ouensanga A. Fourier transform infrared spectroscopic study of thermal degradation of sugar cane bagasse［J］. *Journal of Analytical and Applied Pyrolysis*, 1996, 38（1/2）: 61-73.

(Editor: Zhao Yang)